



Evaluation on Steel Bar Corrosion Embedded in Antiwashout Underwater Concrete

Han-Young Moon¹⁾ and Kook-Jae Shin¹⁾*

¹⁾Dept. of Civil Engineering, Hanyang University, Seoul, 133-791, Korea

(Received, November 10, 2004; Accepted, March 7, 2005)

Abstract

This study aims the evaluation of the corrosion of steel bar embedded in antiwashout underwater concrete, which has rather been neglected to date. To that goal, accelerated steel bar corrosion tests have been performed on three series of steel bar-reinforced antiwashout underwater concrete specimens manufactured with different admixtures. The three series of antiwashout underwater concrete were: concrete constituted exclusively with ordinary portland cement (OPC), concrete composed of ordinary portland cement mixed with fly-ash in 20% ratio (FA20), and concrete with ground granulated blast furnace slag mixed in 50% ratio (BFS50). The environment of manufacture was in artificial seawater.

Measurement results using half-cell potential surveyor showed that, among all the specimens, steel bar in OPC was the first one that exceeded the threshold value proposed by ASTM C 876 with a potential value below -350mV after 14 cycles. And, the corresponding corrosion current density and concentration of water soluble chloride were measured as $30 \mu\text{A}/\text{mm}^2$ and 0.258%. On the other hand, for the other specimens that are FA20 and BFS50, potential values below -350mV were observed later at 18 and 20 cycles, respectively.

Results confirmed the hypothesis that mineral admixtures may be more effective on delay the development of steel bar corrosion in antiwashout underwater concrete.

Keywords : *antiwashout underwater concrete, half-cell potential value, corrosion current density, water soluble chloride*

1. Introduction

Antiwashout underwater concrete is by nature used essentially in aquatic environment and is increasingly finding most of its applications in marine environment rather than fresh water or river. However, differently from structures constructed in fresh water or in river, the structures built under marine environment are showing significant loss of durability and one main reason of such loss is the penetration of Cl^- ion included in seawater. Particularly, Cl^- ions infiltrated inside concrete cause embedded steel bar to corrode and instigate cracks to develop, of which extent affects sensitively the durability of concrete.

Up-to-date, numerous researches have been led to evaluate properties of antiwashout underwater concrete like its

segregation degree, fluidity and compressive strength, but their scope remain limited to basic properties without or with very little regard to its durability. In view of such circumstances, researches on the corrosion of reinforcing bar are thus inexistent.

Since its invention, about 35 years ago in Germany, antiwashout underwater concrete has seen continuous evolution. Sogo et al. in 1987 attempted to increase its resistance against washout by adding polymer.¹⁾ Thereafter, in 1990, Hara et al. succeeded in improving its fundamental properties by mixing of ground granulated blast furnace slag.²⁾ Hara found out that the titrated rate of substitution ranged between 40 and 50%. Especially, Khayat et al. published his first treatise on antiwashout underwater concrete in 1995 followed by many other ones and, contributed greatly to the development of fluidity and self-compacting properties of antiwashout underwater concrete.³⁻⁷⁾ Unfortunately, most of these papers focused essentially on the fundamental

* Corresponding author

E-mail address: rickyshin@hotmail.com

©2005 by Korea Concrete Institute

properties of antiwashout underwater concrete such as fluidity, filling-up performance, and application of mineral additives, neglecting the durability aspect.

With these regards, this study takes place in the framework of durability evaluation of antiwashout underwater concrete. In this study, corrosion tests of steel bar embedded in antiwashout underwater concrete were performed and data were examined. The natural electric potential and the corrosion current density of steel bar were measured during 24 cycles using a half-cell potential surveyor and guard ring device. The amount of soluble chloride and the rate of corroded area were finally calculated and processed.

2. Experimental procedures

2.1 Materials

Ordinary Portland Cement (OPC, type 1) usually manufactured in Korea was used as basic cementitious material, and fly-ash (FA) and ground granulated blast furnace slag (BFS) were employed as supplementary cementitious materials. The chemical compositions and physical properties of cement and mineral admixtures are shown in Table 1. Well-graded crushed stone aggregates and siliceous sand with a fineness modulus of 2.83 were used. Their physical

properties are summarized in Table 2. The liquid-based cellulosic anti-washout underwater admixture (AWA) and the melamine-based high range water reducer (HRWR) presented specific gravities of 0.8 and 1.23, respectively, with the properties listed in Table 3. For the reinforcement, smoothed steel bar with a diameter of 13mm was employed and its chemical composition is given in Table 4. Before being embedded in concrete, the bar was brushed with No. 200 sand paper and cleaned with acetone.

2.2 Preparation of specimen

For the experiments, three series of antiwashout underwater concrete were mixed: (1) concrete constituted exclusively by ordinary portland cement (OPC), (2) concrete composed of ordinary portland cement mixed with fly-ash in 20% ratio (FA20) and (3) concrete in which ground granulated blast furnace slag is mixed in 50% ratio (BFS50). The all specimens were manufactured in artificial seawater, which was a contrived method to consider the real marine circumstance. The cast method of steel bar reinforced anti-washout underwater concrete is schematically shown in Fig. 1 and the details of the specimen are shown in Fig. 2.

To measuring the amount of water soluble chloride, manufactured specimens were coated with epoxy on the

Table 1 Chemical compositions and physical properties of cement and mineral admixtures (%)

	SiO ₂	Al ₂ O ₃	Fe ₂ O ₃	CaO	MgO	SO ₃	Ig. loss	Specific gravity	Specific surface area (cm ² /g)
OPC	21.95	6.59	2.81	60.10	3.32	2.11	2.58	3.15	3,112
FA	67.70	25.00	2.85	2.00	0.90	-	3.47	2.15	3,274
BFS	32.30	14.80	0.40	44.10	5.50	1.00	1.10	2.80	4,580

Table 2 Physical properties of aggregates

	Specific gravity	Absorption (%)	Percentage of solids (%)	F.M.	Abrasion value (%)	Unit weight (kg/m ³)
Fine aggregate	2.59	0.80	56.4	2.83	-	1,473
Coarse aggregate	2.66	0.78	64.9	6.51	28.6	1,741

Table 3 Physical properties of chemical admixtures

	Main composition	Specific gravity	Dosage (%)	Appearance
AWA	HPMC	0.8 ± 0.1	1.0 ~ 1.2 (W×%)	White powder
HRWR	Melamine	1.23 ± 0.02	1.8 ~ 2.1 (C×%)	Transparent liquid

Table 4 Chemical compositions of rebar (%)

C	Si	Mn	P	S	Ni	Cr	Mo	Cu	Sn
0.24	0.23	0.95	0.016	0.008	0.03	0.04	0.01	0.02	0.0005

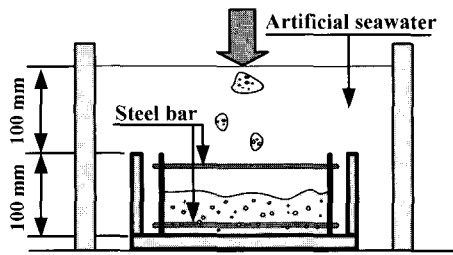


Fig. 1 The manufacture method of steel bar reinforced antiwashout underwater concrete

whole surface excluding the one crossed section, so the unidirectional penetration of chloride was allowed. The measurements of the amount of water soluble chloride were performed after 14 and 24 cycles of test. The mixture proportions adopted for each series are listed in Table 5. All specimens were taken out from those molds after 48 hours, followed by standard curing until the next test.

2.3 Test techniques

2.3.1 Accelerated corrosion test

For the accelerated corrosion test, 2X concentration of artificial seawater based on ASTM D 1141 was employed. After 14 days of standard curing, the specimens were immersed for 3 days in 2X concentration of artificial seawater and dried for 4 days at ambient temperature. The test was conducted for 24 cycles and 1 cycle was readjusted with 3 days of wetting and 4 days of drying.

2.3.2 Half-cell potential test

In conformity with ASTM C876, the corrosion potential (E_{corr}) was measured by means of half-cell potential surveyor. The reference electrode (RE) was provided by a saturated copper sulfate electrode (CSE). Fig. 3 schematizes the test method using half-cell potential surveyor.

2.3.3 Corrosion current density

A guard ring device was used to measure I_{corr} since Strategic Highway Research Program (SHRP) has recognized the reliability of its performance.⁸⁾

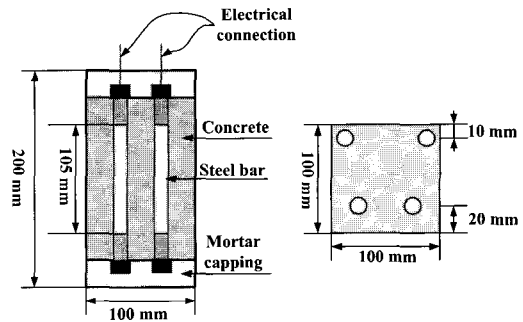


Fig. 2 Schema of steel rebar corrosion specimen

The process of the test method, illustrated in Fig. 4, is very similar to half-cell potential surveyor.

2.3.4 Amount of water soluble chloride

Prepared specimens were drilled at various locations to produce powdered samples that were collected. Then, according to the recommendations of the Japan Concrete Engineering Association related to the evaluation procedure of salt content in reinforced concrete, salt solution is extracted so as to measure the ratio of cement weight and chloride amount (Cl^- %) with the chloride ion detector using selective ion electrode.

2.3.5 Rate of corrosion area

After 24 cycles, the steel bar embedded in antiwashout underwater concrete is taken out and the rusted portions are scratched on tracing paper. Using a plotting paper, the rate of corrosion area is calculated with Eq. (1) where n is the number of intersection points in corroded portion and N is the total number of intersection points included in the development figure of the steel bar.

$$\text{Rate of corrosion area}(\%) = \frac{n}{N} \times 100 \quad (1)$$

3. Results and discussion

3.1 Electrochemically measured E_{corr} and I_{corr}

Fig. 5 illustrates the values of E_{corr} in each cycle for OPC, FA20 and BFS50. All the tested specimens showed distinctive

Table 5 Mixture proportions of each series

	W/Cm (%)	S/a (%)	Air (%)	Unit weight (kg/m ³)						AWA (W X %)	HRWR (C X %)
				W	C	G	S	FA	BFS		
OPC	50	42	4±1	210	420	938	674	-	-	1.20	1.80
FA20	50	42	4±1	210	336	918	660	84	-	1.20	1.80
BFS50	50	42	4±1	210	210	924	664	-	210	1.20	1.80

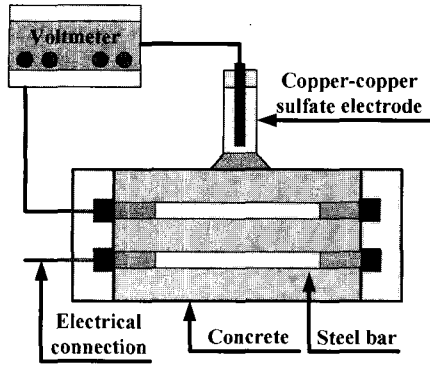


Fig. 3 Schematic details of the half-cell potential test

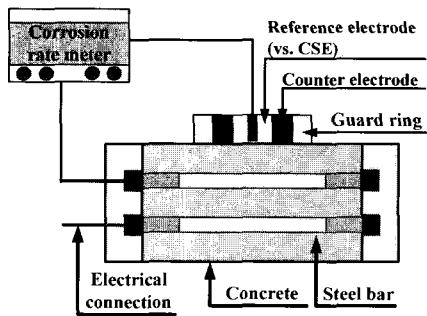


Fig. 4 Schematic details of guard ring device test

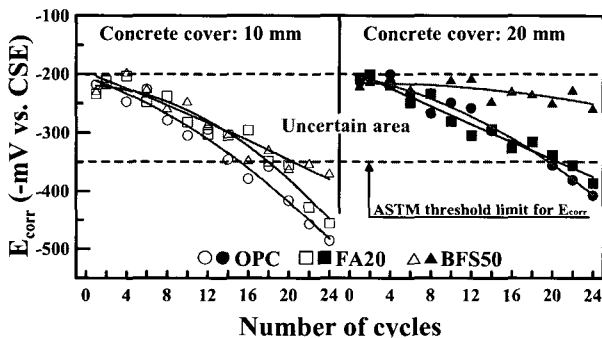


Fig. 5 E_{corr} vs. number of cycles

threshold values of corrosion for 10 mm and 20 mm of concrete cover. If the corrosion threshold potential value of steel bar is -350mV , CSE (with respect to copper/copper sulfate electrode) as proposed by ASTM C 876, the reinforcing bar with 20mm of concrete cover exhibits the most stable potential value range ($-200 \sim -350\text{mV}$), compared to 10mm of concrete cover. As a matter of fact, increasing the thickness of concrete cover is the best solution to slow down corrosion. However, this method is out-of-date being economically onerous.

On the other hand, as shown in Fig. 5, potential below -350mV began to appear after 14 cycles (98days) for OPC

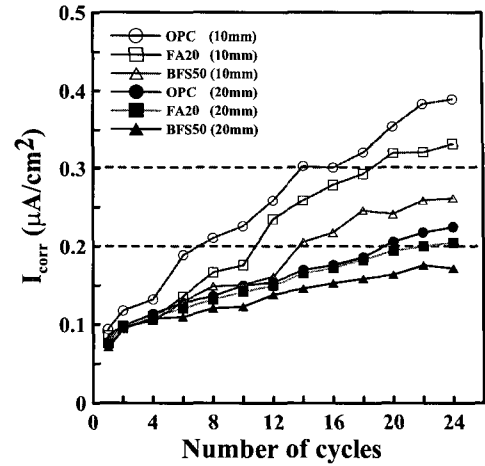


Fig. 6 I_{corr} vs. number of cycles

specimen with concrete cover of 10mm. This specimen was the first one to exceed the corrosion threshold potential. Meanwhile, the potential value below -350mV for FA20 and BFS50 was observed at 18 cycles (126days) and 20 cycles (140 days), respectively. With this regard, the starting point of corrosion may thus be delayed in some extent by the mineral admixtures.

Similar results were obtained for the corrosion current density summarized in Fig. 6. The slope of corrosion current density tends to become lower successively for OPC, FA20 and BFS50. At 14 cycles, corresponding to the time when potential becomes lower than -350mV in steel bar with 10 mm of concrete cover, the corrosion current densities of OPC, FA20 and BFS50 approach 30, 26 and $20 \mu\text{A}/\text{mm}^2$, respectively. According to the Strategic Highway Research Program (SHRP), it is reported that when corrosion current density ranges between $20 \mu\text{A}/\text{mm}^2$ and $50 \mu\text{A}/\text{mm}^2$, the corrosion has begun or is going to begin. Several researchers have considered values of current density greater than $30 \mu\text{A}/\text{mm}^2$ to be indicative of active corrosion.^{9,10} Andrade and Alonso have provided a set of value for the levels of corrosion rate. They considered that corrosion current density of 10 to $50 \mu\text{A}/\text{mm}^2$ is low and 50 to $100 \mu\text{A}/\text{mm}^2$ is moderate. Values above $100 \mu\text{A}/\text{mm}^2$ are considered high while below $10 \mu\text{A}/\text{mm}^2$ are deemed negligible.^{11,12} Gonzalez et al¹¹ concluded that corrosion current density less than 10 to $20 \mu\text{A}/\text{mm}^2$ would be acceptable with no durability risks.

Consequently, even if the more conservative value of 20 is adopted, OPC and FA20 already exceeded the corrosion threshold value and BFS50 just reached the corrosion threshold value. However the half-cell potential values of FA20 and BFS50 measured at 14 cycles were -305mV and -302mV , respectively, and did not exceed the corrosion threshold limit proposed by ASTM C 876 (Fig. 5). Hence, it

is verified that more moderate value of $30\mu\text{A}/\text{mm}^2$ is more acceptable to evaluate steel bar corrosion of antiwashout underwater concrete. In conformity with Al Amoudi et al,¹⁰ it can be concluded the value $30\mu\text{A}/\text{mm}^2$ is more appropriate for the threshold value for reinforcement corrosion.

The relationship between corrosion current density and half-cell potential value during the cycles of exposure to accelerated corrosion test is shown in Fig. 7. It is seen here that a current density of 20 and $30\mu\text{A}/\text{mm}^2$ is associated with the half-cell potential threshold value of -350mV , CSE. From the results in Fig. 7, a relationship between corrosion current density (I_{corr}) and half-cell potential (E_{corr}) for OPC with concrete cover of 10 mm could be expressed as:

$$I_{\text{corr}} = 0.342 \times \ln(E_{\text{corr}}) - 1.712 \quad (2)$$

Within 24 cycles (168 days) of accelerated corrosion test, corrosion current density reaching almost $40\mu\text{A}/\text{mm}^2$ could be predicted from Eq. (2) only for OPC-based antiwashout underwater concrete. On the other hand, Fig. 7 shows that corrosion current density and half-cell potential value for BFS50 remained at a relatively low level throughout the testing periods. It should be stressed that the special ingredients for durable antiwashout underwater concrete such as ground granulated blast furnace slag may result in particular effects on performance.

3.2 Soluble chloride contents

The “water soluble” chloride ion penetration profile of antiwashout underwater concrete manufactured under artificial seawater is illustrated in Fig. 8. After 14 cycles, the water soluble chloride value of OPC at 10mm from the surface exceeded the critical limit of 0.15% proposed by ACI 318-99 for water soluble chloride content, and the concentration of water soluble chloride at 10mm steel depth approached 0.258%. In other words, this means that corrosion of steel bar has already proceeded to some extent in conformity with ACI 318-99. However, recalling the results of Fig. 5, it has been seen that the half-cell value of OPC with 10 mm of concrete cover barely reached -350mV , CSE after 14 cycles. This means that it has only arrived to the potential threshold value for high probability of corrosion activity, which is -350mV , CSE with respect to copper/copper sulphate electrode.^{13,14} The corresponding corrosion current density can be observed in Fig. 6. As mentioned above, the corrosion current density of OPC with 10mm concrete cover at 14 days was about $30\mu\text{A}/\text{mm}^2$. This result means that the test result is about to reach the threshold value if the moderate value is assumed as $30\mu\text{A}/\text{mm}^2$ as discussed above. Consequently, 0.15% proposed by ACI 318-99 may

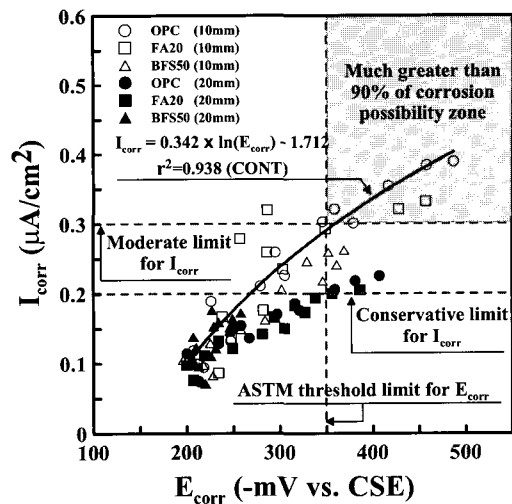


Fig. 7 I_{corr} vs. E_{corr} for specimens cast in artificial seawater

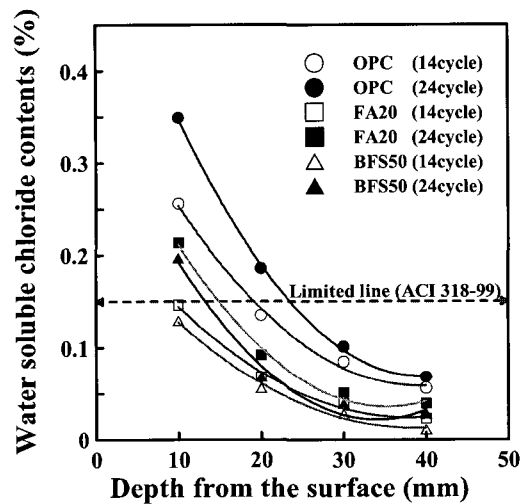


Fig. 8 Chloride concentration profile and regression curves

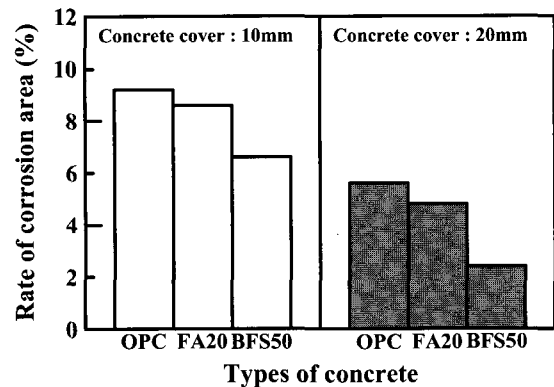


Fig. 9 Rate of corrosion area

be seen to be slightly conservative for critical limit of anti-washout underwater concrete.

Water soluble chloride contents measured at 14 cycles were 0.146% and 0.129% in antiwashout underwater concrete prepared by mixing fly-ash and ground granulated blast furnace slag, respectively. This can be explained by the fact that fly-ash and ground granulated blast furnace slag induce pozzolan reaction and potential hydraulic property and so-generated compact C-S-H hydrates fill the capillary pore which is the main migration channel of chloride.

3.3 Rate of corrosion area

After 24 cycles, steel bar in each specimen were taken out and the rate of corrosion area were calculated according to Eq. (1). As shown in Fig. 9, the rate of corrosion area runs around 9.2% in OPC with 10mm of concrete cover and, approaches 8.6% and 6.6% in FA20 and BFS50, respectively. This result is consistent with electrochemical and water soluble chloride content measurements. Thus, that is to say, special ingredients for durable antiwashout underwater concrete such as ground granulated blast furnace slag and fly ash may result in particular effects on performance. Especially, according to the overall results, ground granulated blast furnace slag showed more outstanding performance.

4. Conclusions

- 1) From the accelerated corrosion test, it was observed that the first one to exceed the threshold value, below -350mV proposed by ASTM C 876, was the steel bar embedded in OPC with 10mm thick concrete cover after 14 cycles, but as for FA20 and BFS50, the potential value below -350mV was observed at 18 and 20 cycles, respectively. This verified that mineral admixtures retarded the development of corrosion in steel bar.
- 2) When potential value below -350mV were observed at 14 cycles, the corrosion current densities measured in steel bar embedded in OPC, FA20 and BFS50 were $30\mu\text{A}/\text{mm}^2$, $26\mu\text{A}/\text{mm}^2$ and $20\mu\text{A}/\text{mm}^2$, respectively. The corresponding potentials of FA20 and BFS50 were -305mV and -302mV, respectively, which did not reach the threshold value. Following, the threshold value of $30\mu\text{A}/\text{mm}^2$ can be considered as an acceptable value when evaluating the corrosion state of steel bar-reinforced antiwashout underwater concrete by means of corrosion current density measured by guard ring device. Nevertheless, deeper researches are needed to correlate field and laboratory results.

- 3) The amount of soluble chloride measured at 14 cycles for OPC at a depth of 10 mm was 0.258%, which exceeds 0.15%, the value prescribed in ACI 318-99, by 0.108%. This means that corrosion of steel bar has already proceeded to some extent. However, it has been seen that the corresponding of half-cell value barely reached -350mV and the corrosion current density was about $30\mu\text{A}/\text{mm}^2$. Consequently, 0.15% proposed by ACI 318-99 may be slightly conservative for critical limit of antiwashout underwater concrete. On the other hand, the amount of soluble chloride measured for FA20 and BFS50 at 10mm depth was measured as 0.146% and 0.129%, respectively.
- 4) After completion of the planned experiments, for 24 cycles, the rate of corrosion area of 9.2% in OPC with 10 mm depth was obtained and, 8.6% and 6.6% in FA20 and BFS50, respectively. This confirms the hypothesis that ground granulated blast furnace slag and fly ash are effective in increasing the resistance of steel bar-reinforced antiwashout underwater concrete against steel bar corrosion.

Acknowledgement

This study has been a part of a research project supported by Korea Ministry of Construction and Transportation (MOCT) via the Infra-Structures Assessment Research Center. The authors wish to express their gratitude for the financial support.

References

1. Sogo, S., Haga, T., and Nakagawa, T., "Underwater Concrete Containing Segregation Controlling Polymers," *5th International Congress on Polymers in Concrete*, Brighton, England, September, 1987.
2. Hara, M., *Admixing Effect of High Fineness Slag on the Properties of Underwater Concrete*, Admixtures for Concrete, Improvement of Properties, E. Vazquez, editor. Chapman & Hall, London.
3. Khayat, K. H., "Effects of antiwashout admixtures of fresh concrete properties," *ACI Materials Journal*, Vol. 92, No.2, 1995, pp.164~171.
4. Khayat, K. H., "Effects of antiwashout admixtures on properties of hardened concrete," *ACI Materials Journal*, Vol.93, No.2, 1996, pp.134~146.
5. Sonebi, M. and Khayat, K. H., "Effect of mixture composition on relative strength of highly flowable underwater concrete," *ACI Materials Journal*, Vol.98, No.M26, 2001, pp.233~239.

6. Khayat, K. H. and Sonebi, M., "Effect of mixture composition on washout resistance of highly flowable underwater concrete," *ACI Materials Journal*, Vol.98, No. M31, 2001, pp.289~295.
7. Khayat, K. H. and Joseph, Assaad, "Relationship between washout resistance and rheological properties of high-performance underwater concrete," *ACI Materials Journal*, Vol.100, No.M21, 2003, pp.185~193.
8. Janusz, F., Akshey, S., Dan Li, and Philip, D. Cady, *Condition Evaluation of Concrete Bridges Relative to Reinforcement Corrosion*, Vol.2: Method for Measuring the Corrosion Rate of Reinforcing Steel, SHRP-S/FR-92-104, Strategic Highway Research Program, National Research Council, Washington, DC, USA, 1992, pp.17~27.
9. Andrade, C., Alonso, C., and Gonzalez, J. A., *An initial effort to use corrosion rate measurements for estimating rebars durability*, In: Berke, N. S., Chaker, V., Whiting D., editors., *Corrosion rates of steel in concrete*, ASTM STP 1065, Philadelphia: American Society for Testing and Materials; 1990. pp.29~37.
10. Al-Amoudi OSB, Maslehuddin, M., Lashari, A. N., and Almusallam, A. A., "Effectiveness of corrosion inhibitors in contaminated concrete," *Cement & Concrete Composites*, Vol.25, No.4-5, 2003, pp.439~449.
11. Gonzalez, J. A., Feliu, S., Rodriguez, P., Ramirez, E., Alonso, C., and Andrade, C., "Some questions on the corrosion of steel in concrete-Part I: when, how and how much steel corrodes," *ACI Material Structures*, 1996, Vol.29 (Jan.-Feb.), pp.40~46.
12. Andrade, C. and Alonso, C., "On-site measurements of corrosion rate of reinforcements," *Construction Building Materials*, Vol.15, No.2-3, 2001, pp.141~145.
13. Broomfield, J. P., Angular, A, Sagues, A, A, and Powers, R. G., *Corrosion measurements of reinforcing steel in partially submerged concrete slabs*, In: Berke NS, Chaker V, Whiting D, editors. *Corrosion rates of steel in concrete*, ASTM STP 1065, Philadelphia: American Society for Testing and Materials; 1990. pp.66~85.
14. Baweja, D., Roper, H., and Sirivivatnanon, V., *Specification of concrete for marine environments: a fresh approach*, In: The Australia-US workshop on high performance concrete. Perth: Curtin University; 1997, pp. 411~422.